CONF-77-142-E
E-0398
(Preprint # 30,710)
RECEIVED
FEB 13 1978
DIRECTORS OFFICE
FERMILAB
#398

SCALING PARAMETERS IN DEEP INELASTIC MUON SCATTERING*+

W. R. Francis
Michigan State University, East Lansing, MI 48824

ABSTRACT

In this paper new and still preliminary measurements of the nucleon structure function derived from muon scattering experiments at Fermilab are presented. The data are displayed in such a way as to emphasize the departures from exact Bjorken scaling. Parameters describing the scale breaking are extracted from simple power law fits to the data.

INTRODUCTION

This talk shall be concerned primarily with the presentation of two new determinations of the nucleon structure function carried out at the Fermi National Accelerator Laboratory over the past year. New data are available from E398, the Chicago-Harvard-Illinois-Oxford Collaboration[1] (CHIO) of which I am a member, measuring inclusive muon scattering from hydrogen,

$$\mu + p \rightarrow \mu + X, \tag{1}$$

and from E319, the Michigan State University-Fermilab Collaboration[2] (MSU-F), studying the similar process from an iron-scintillator target calorimeter,

$$\mu + \text{Nucleus} \rightarrow \mu + X. \tag{2}$$

Both data sets are preliminary results.

NOTATION

At a fixed beam energy, E, one can specify the kinematics of muon inclusive scattering with two variables, for example, the two traditional variables Q^2 and ν, the momentum transfer squared and laboratory energy loss of the muon. Alternatively one can choose simple scaled variables x ($=Q^2/2M\nu=1/\omega$) and y ($=\nu/E$). Here M is the target nucleon mass.

The physics of this scattering process can be parameterized in terms of two functions which contain the strong interaction dynamics of interest.

*Research supported by the National Science Foundation
+Invited talk presented by W. R. Francis at the Argonne Meeting of the American Physical Society Division of Particles and Fields, October 6-8, 1977.

$$E\,\frac{d^2\sigma}{dxdy} = \frac{4\pi\alpha^2}{2M}\;\frac{F_2\,(X,Q^2)}{x^2y^2}\left[1 - y + \frac{y^2}{2\,(1 + R\,(X,Q^2))}\right]. \quad (3)$$

Here we have chosen these functions to be F_2 $(=\nu W_2)$ the nucleon structure function, and R, the "well-known" ratio of total absorption cross sections of longitudinal and transverse virtual photons.

Compare this to the cross section for muon scattering from the electron,

$$E\,\frac{d^2\sigma}{dxdy} = \frac{4\pi\alpha^2}{2m}\;\frac{\delta(x-1)}{x^2y^2}\left[1 - y + \frac{y^2}{2}\right]. \quad (4)$$

The similarity of form is due solely to the one-photon exchange approximation to the electromagnetic part of the interaction.

HISTORY

As everyone here knows, it was found in the first measurements of this process by the SLAC-MIT[3] group that

$$F_2\,(X,Q^2) \approx F_2\,(X) \text{ and}$$
$$R\,(X,Q^2) \approx \text{small}. \quad (5)$$

The strong interactions imitate scattering from point-like, spin-1/2 particles to a great degree, hinting broadly at the existence of such constituents within the nucleon. The complete independence of F_2 on Q^2, predicted at infinite Q^2 by Bjorken[4], is known as scaling. In this talk the observed deviations from scaling will be discussed in some detail but from a point of view which has changed substantially from that used in the first approaches to this subject.

Violations of exact scaling have always been known to exist but were initially regarded as principally due to finite Q^2 effects which should not be allowed to detract from the really remarkable degree to which scaling was approximated at the rather low values of momentum transfer squared accessible to experimenters. Pursuing this theme, much time was expended in the study of approaches to scaling and in searches for "better" scaling variables[5] - variables asymptotically equivalent to x but removing or lessening the observed scaling deviations at finite values of Q^2.

This view changed abruptly with the appearance of the first muon scattering results from Fermilab.[6] The high beam energy allowed expansion of the accessible kinematic range by a full decade in both Q^2 and ν. The simple changes of variable designed to minimize scaling deviations at low energies failed to remain effective over the much larger kinematic region, revealing scale breaking as a genuine, high-Q^2 effect.

SCALE BREAKING PARAMETERS

The departures from exact scaling are fairly small. Equivalently, the dependence of $F_2(X,Q^2)$ on Q^2 is quite weak. It has become common to parameterize this dependence through the parameter

$$b(x) = \frac{d(\log F_2)}{d(\log Q^2)} . \tag{6}$$

This implies a power law form for the structure function

$$F_2\ (X,Q^2) = F_2\ (X,Q_o^2)\ \left(\frac{Q^2}{Q_o^2}\right)^{b(x)} \tag{7}$$

which is similar to the behavior of so-called conventional field theories when the ideas of renormalization group theory[7] are applied. Here Q_o^2 is any reference point, usually chosen in the range 2 to 3 GeV^2.

It is probably worthwhile to point out that this equation can be rewritten as

$$F_2\ (X,Q^2) = F_2\ (X,Q_o^2)\ \exp\ \left(b(x)\ \log \frac{Q^2}{Q_o^2}\right) \tag{8}$$

and approximated to read

$$F_2\ (X,Q^2) \simeq F_2\ (X,Q_o^2)\ \left(1 + b(x)\ \log \frac{Q^2}{Q_o^2}\right) \tag{9}$$

if Q^2 is near Q_o^2 and/or $b(x)$ is small. This last is more like the form one might expect from the popular non-Abelian gauge theories.[8] The point is that, since $b(x)$ is small and the range in $\log Q^2$ is not large, a choice between these two alternatives based only on these data is not possible.

A second common way of parameterizing the scaling violations involves an attempt to summarize all effects in a single number, a.

$$a = \frac{d\ (\log F_2)}{d(\log \frac{Q^2}{Q_o^2})\ d(\log \frac{\omega^2}{\omega_o^2})} . \tag{10}$$

This corresponds to

$$b(x) = -\ a\ \log 6x \tag{11}$$

where I have chosen $\omega_o=6$ as the point where $b(x)$ changes sign.

This parameterization is, of course, more restrictive than the former (one variable as opposed to one function) and, as we shall see, fails to describe the data well near the kinematic boundaries $x=0$ and $x=1$.

CHIO - EXPERIMENT 398

Figure 1 is a plan view of the CHIO apparatus. Positively charged muons with a mean energy near 219 GeV are directed onto a 1.2 meter long liquid hydrogen target. The scattered muons are

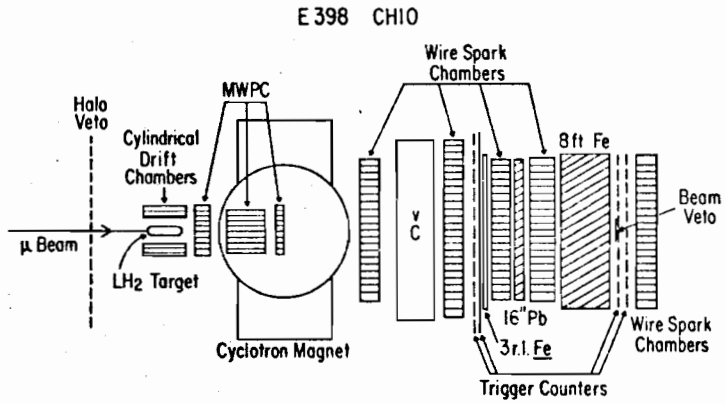

Fig. 1. Plan view of the CHIO apparatus.

measured in one meter square multiwire proportional chambers immediately downstream of the target, momentum analyzed with the 2.3 GeV transverse momentum kick of the Chicago cyclotron magnet, measured again in the 2 by 6 meter wire spark chambers downstream of this magnet, and, finally, identified by passing through the old Rochester cyclotron which has been cut up to provide an iron wall approximately 8 feet thick. Although this aspect of the data will not be discussed here today, this apparatus also observes nearly the entire hadronic final state.

The experiment trigger demands only that a muon leave the beam. This can happen either by the muon suffering a large energy loss ($\nu \gtrsim 160$ GeV) in which case the muon is swept out of the beam by the analyzing magnet or by the muon experiencing a large angle scatter ($\theta_\mu \gtrsim 10$ mrad.) in which case the muon leaves the beam under its own power. Figure 2 shows the region of the Q^2-ν plane where the acceptance is good, that is, between about 20 and 100%. Although the acceptance remains large out to quite high values of Q^2, the region with significant numbers of events ends somewhere between Q^2's of 50 and 100 GeV^2 as indicated roughly by the dotted line.

The analysis details are not particularly exciting and will not be presented in any detail here except for a brief mention of the quantity R. As Equation 3 makes clear, extraction of F_2 (X,Q^2) from the measured cross sections requires some knowledge of the other unknown function R (X,Q^2). Since CHIO does have data taken at three different beam energies, measurements of R do exist in some kinematic regions. These measurements[9], however, are low in precision serving mainly to substantiate, at high ν, the low energy result that R is not large.

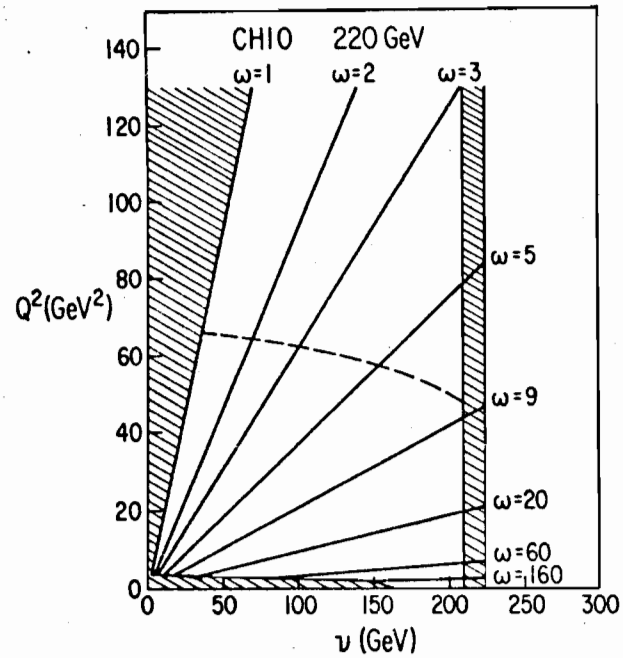

Fig. 2. Kinematic acceptance of the CHIO apparatus for 220 GeV incident muons.

This imprecision is due primarily to the fact that, over most of the kinematic region, the cross section depends only extremely weakly on R. Taking advantage of this last, it was decided that, until measurements of R were better defined, F_2 (X,Q^2) could be extracted most simply and still accurately by assuming a constant value as determined by the low energy experiments. At the time that the present analysis was performed the best such average R was the MIT-SLAC measurement[10] $\bar{R} = 0.14 \pm 0.12$. All results presented here have this as an input.

At the recent Hamburg meeting the results of a new determination of R by the SLAC Group A[11] were presented indicating $\bar{R} = 0.35 \pm 0.16$. Combining these two independent measurements yields a new best estimate $\bar{R} = 0.25 \pm 0.10$. Reanalysis of the CHIO data with this new $\bar{R}$ input would raise most measured values of F_2 by 1% or less, an amount considerably smaller than the estimated statistical errors. A few points at high y would increase by 1 to 10%, approximately one standard deviation in the worst case. The effects on the scale breaking parameters are, accordingly, extremely small.

CHIO - RESULTS

The results presented here are preliminary but not too preliminary. By this is meant the following. The previous CHIO experiment, E98, has finalized and published cross section measurements at muon beam energies of 96 and 149 GeV. The current

219 GeV results, although still being carefully checked, agree quite well where there is overlap. This point is illustrated in Figure 3. Here old and new data are compared for two extremely

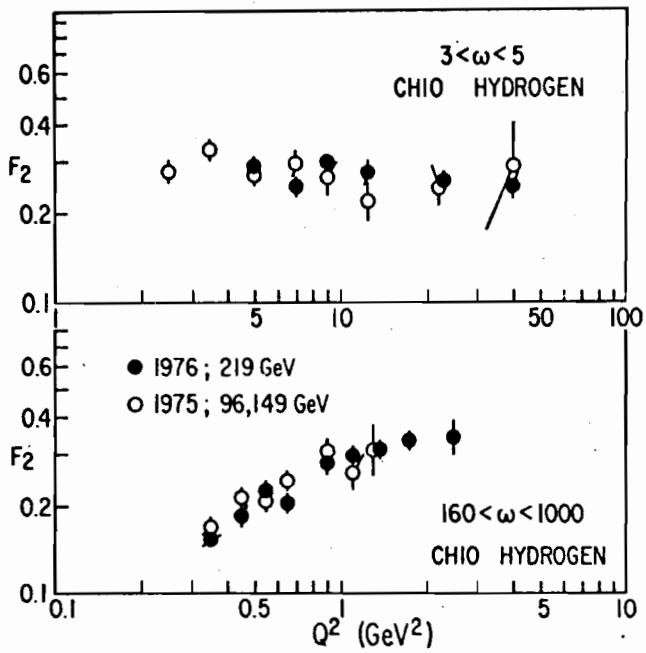

Fig. 3. Comparison of old and new CHIO results.

different regions of ω and Q^2. This agreement is typical. A chi-squared type comparison of the two data sets gives a value of 169 for 143 data points. In view of this good agreement the data from all three beam energies have been combined to study the scale breaking effects with the highest precision.

Figures 4 through 7 present plots of log F_2 versus log Q^2. A power law fit (Equation 7) gives a straight line whose slope is the scale breaking parameter b. In Figures 4 through 6 this fit is made only for points with $Q^2 > 2$ GeV^2. The familiar pattern emerges. For $\omega < 6$, the structure function decreases with increasing Q^2, the rate of decrease being quite large near the kinematic limit $\omega = 1$. Near $\omega = 6$, the sign of the scaling violation changes. For $\omega > 6$, F_2 rises with Q^2.

Figure 7 presents very high ω data. Here the kinematics severely restrict the maximum possible value of Q^2. Accordingly, the fitting range has been extended to include points with Q^2 as low as 1 GeV^2. Clearly, F_2 still increases with Q^2 but it is difficult at these low values of momentum transfer squared to separate reliably the power law scaling violations from the more trivial, expected rise from the kinematic zero possessed by F_2 (X,Q^2) at $Q^2 = 0$.

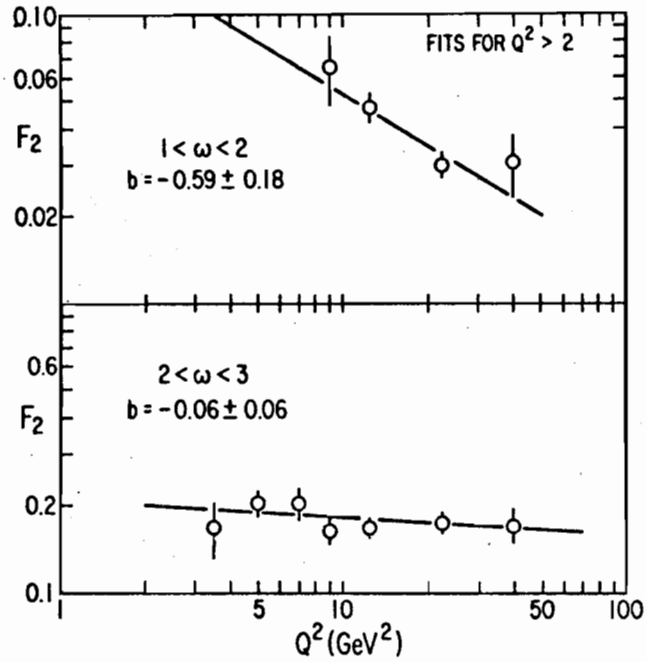

Fig. 4. CHIO Hydrogen data.
Scale breaking parameters.

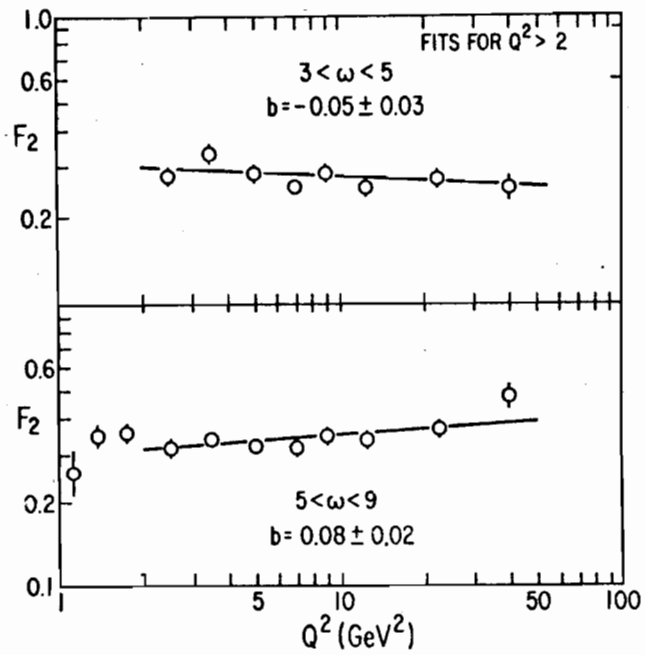

Fig. 5. CHIO Hydrogen data.
Scale breaking parameters.

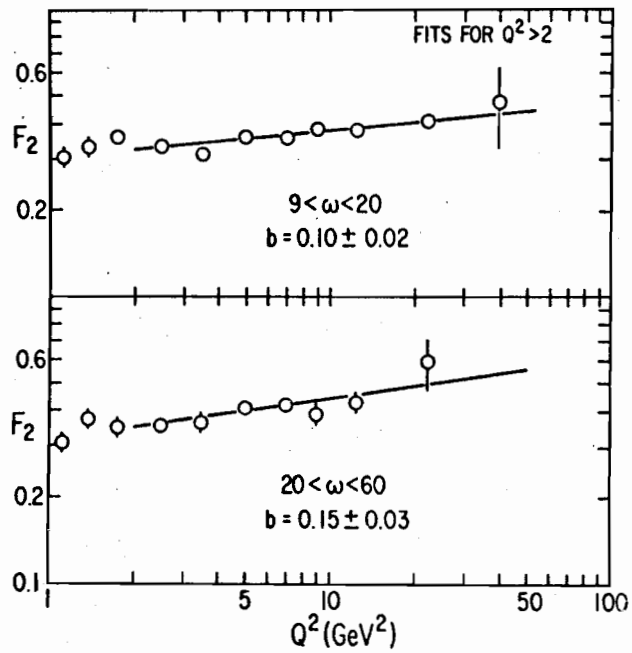

Fig. 6. CHIO Hydrogen data.
Scale breaking parameters

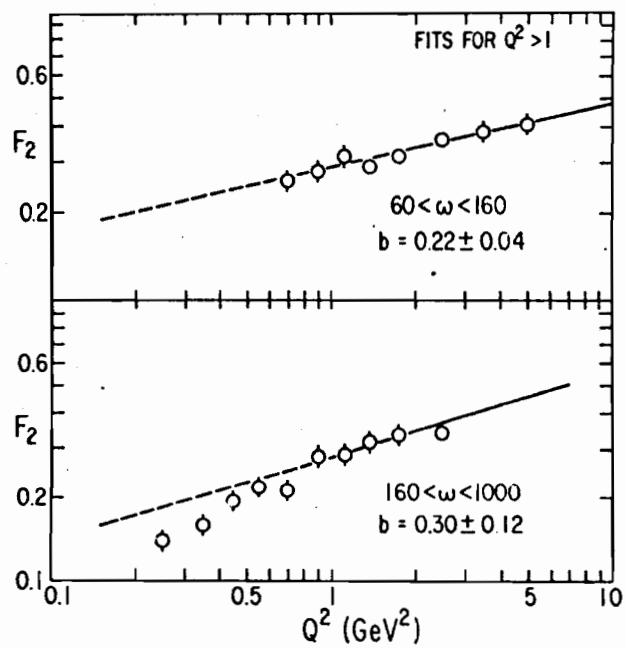

Fig. 7. CHIO Hydrogen data.
Scale breaking parameters

A simple parameterization of this kinematic rise from the $Q^2 = 0$ point used previously to study scaling behavior in the high ω region involved approximating the turn-on with a factor depending only on Q^2,[12]

$$F_2\ (X,Q^2) \equiv \left[1 - F_2^{el}\ (Q^2)\right] G_2\ (X,Q^2). \qquad (12)$$

Here $F_2^{el}\ (Q^2)$ is the analog of F_2 in the elastic scattering process

$$F_2^{el}\ (Q^2) = \frac{G_E^2\ (Q^2) + \tau G_M\ (Q^2)}{1 + \tau}\ ;\ \tau = \frac{Q^2}{4_M{}^2} \qquad (13)$$

where G_E and G_M are, respectively, the elastic electric and magnetic form factors for the proton. Although the applicability of the physics motivating this form is questionable, it does seem to approximate well the observed kinematic rise.

In Reference 12, G_2 was considered Q^2 independent, but here we may expect to see some residual scale breaking of the power law type remaining. Figure 8 presents log G_2 versus log Q^2

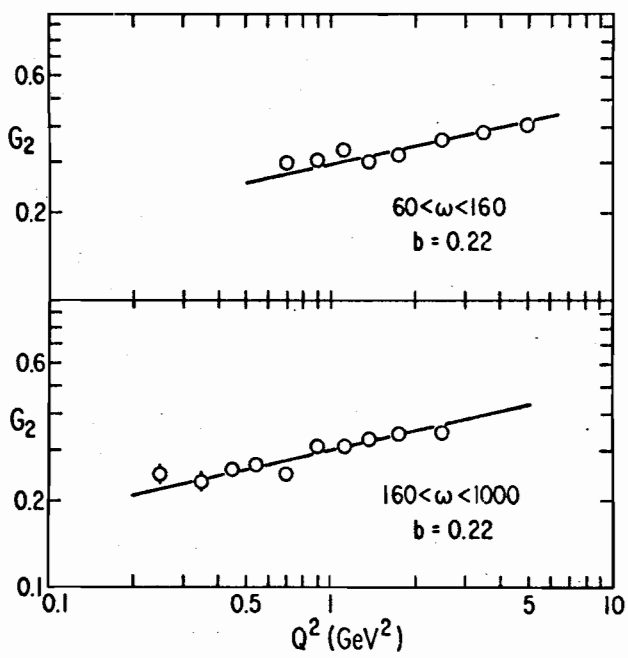

Fig. 8. CHIO Hydrogen data. High ω, low Q^2 region. An attempt has been made to remove some of the kinematic effects at low Q^2.

for the same two high ω regions as Figure 7. Plots in other bins of ω remain essentially unchanged since the kinematic factor is very close to 1 for $Q^2 > 1$ GeV^2. The straight lines appearing

are not best fits to these modified structure functions but are instead the same fit to the $60<\omega<160$ data shown in Figure 7. The very low Q^2 points have moved up much closer to the power law straight lines making it more clear than before that the parameter b is not changing particularly rapidly in the high ω region.

In Figure 9 the present CHIO measurements of the b parameter are collected and compared to the lower energy electron data.[10] Also appearing on this graph are two curves which require some explanation.

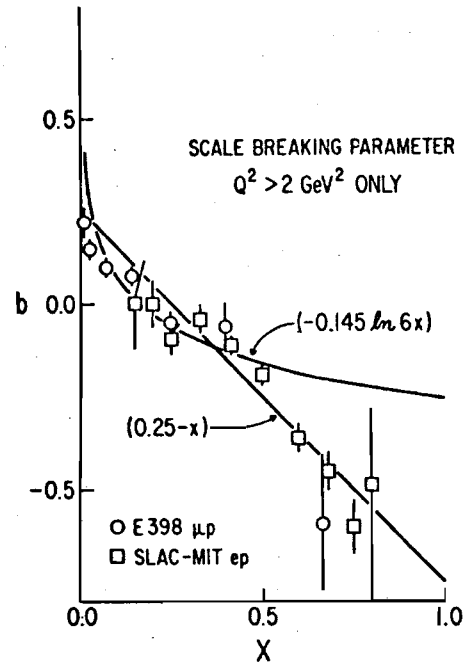

Fig. 9. Hydrogen scale breaking parameters.

The logarithmic curve is the previously mentioned (Equations 10 and 11) attempt to summarize the scaling violations with the single parameter a. The particular value of a shown here is the result of fits to the old CHIO data at 149 and 96 GeV. This parameterization of the scale breaking is clearly a bad approximation at both large and very small x.

The straight line is a curve which I first saw in a paper by Perkins, Schreiner, and Scott.[13] It is not physically motivated but does have the virtues of being simple and easy to remember as well as being a fair representation of the results.

MSU-F - EXPERIMENT 319

Figure 10 is a diagram of the MSU-F apparatus. Muons with mean energy near 275 GeV are incident upon a calorimeter target composed of 4123 g/cm^2 of iron and 108.2 g/cm^2 of scintillator. (Compare this to the 8.4 g/cm^2 liquid hydrogen target of CHIO.) Muons

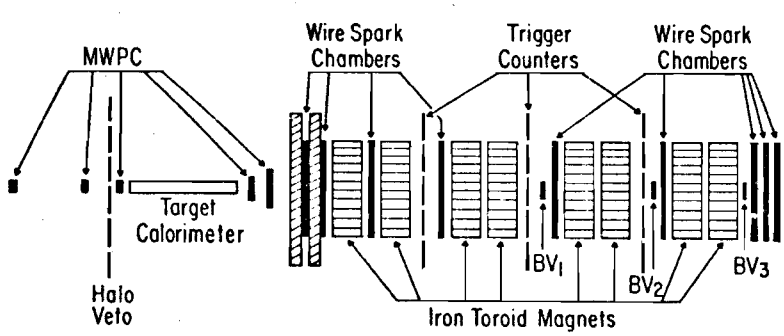

Fig. 10. Plan view of the MSU-F apparatus.

emerging from the calorimeter are measured in multiwire proportional chambers immediately downstream of the target and then momentum analyzed and identified with a spectrometer composed of 8 iron toroidal magnets interspersed with 9 wire spark chambers and 3 planes of scintillation counters. The total energy of the produced hadrons is measured in the calorimeter target, but they are not otherwise individually detected.

The apparatus detects muons emerging from the target at angles between 10 and 100 mrad. At present, for the purpose of evaluating the single muon inclusive scattering cross section, the scattered muon is required to have an energy above 30 GeV. Given a 275 GeV beam and these restrictions, the kinematic region displayed in Figure 11 is accessible. This 30 GeV minimum

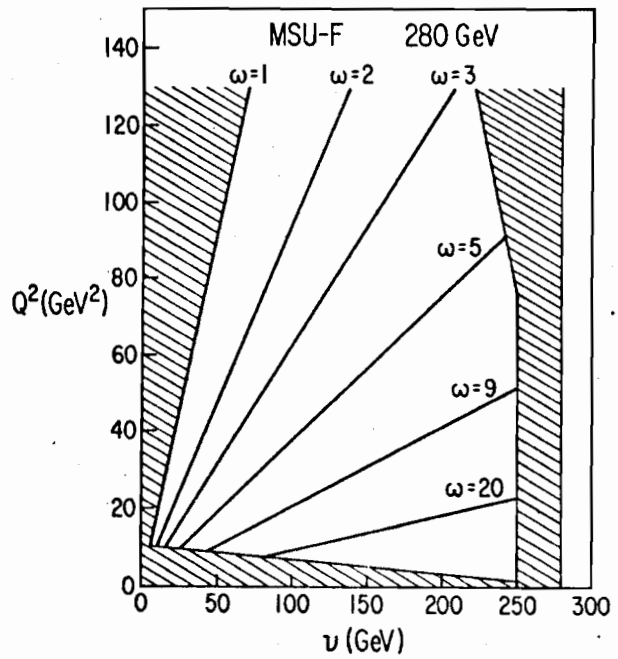

Fig. 11. Kinematic acceptance of the MSU-F apparatus for 280 GeV incident muons.

energy requirement for muon identification can be relaxed to as low as 8 GeV, but this is more important to the other major goal of this experiment, the measurement of the properties of multi-muon final states.

Again, the analysis will not be discussed in detail here except for a few points. F_2 (X,Q^2) is extracted from the measured cross section using a parameterization of R from lower energy electron data,[14] $R = 0.52M^2/Q^2$. Given the insensitivity of the cross section to reasonable choices of R, this certainly imposes no barrier to comparisons with the CHIO results. What is important is the difference in target materials.

Before the MSU-F data, which is mostly scattering from iron, can be compared to the CHIO results, allowance must be made for the known neutron-proton differences[12] which are most important at large x. The CHIO data must be multiplied by a factor of 0.64 at x = 0.67 but only by 0.92 at x = 0.14.

In addition, the radiative corrections differ significantly at low x where, for iron, the correction can become quite large due to coherent scattering effects. For iron this correction is $\sim$ 15% at ω near 50, but always less than 3% for $\omega < 20$.

MSU-F - RESULTS

The primary results are presented in Figures 12 through 16 where measurements of F_2 (X,Q^2) are displayed for 5 different Q^2 bins. These are the same data presented at Hamburg except that the CHIO points have been updated to include the recent results. The solid line appearing in each graph labeled "FIT_{98}" is a fit to the published CHIO data (Experiment 98). It includes scale breaking effects in the approximation that $b(x)=-0.145 \ln(6x)$ and has been "corrected" to include neutron-proton differences.

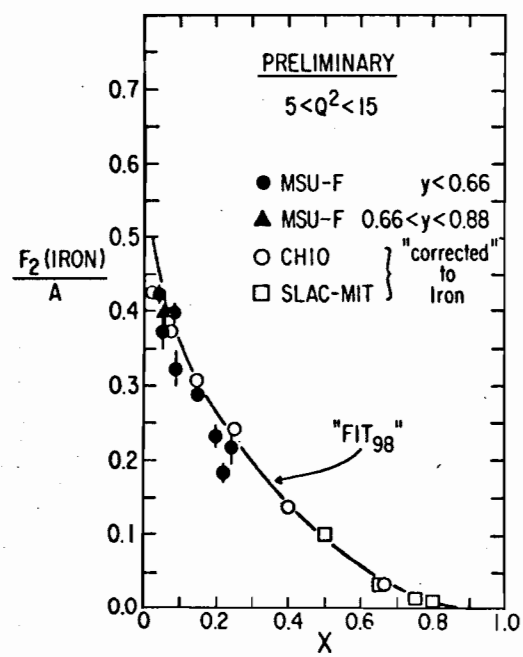

Fig. 12. MSU-F data. Structure function per nucleon.

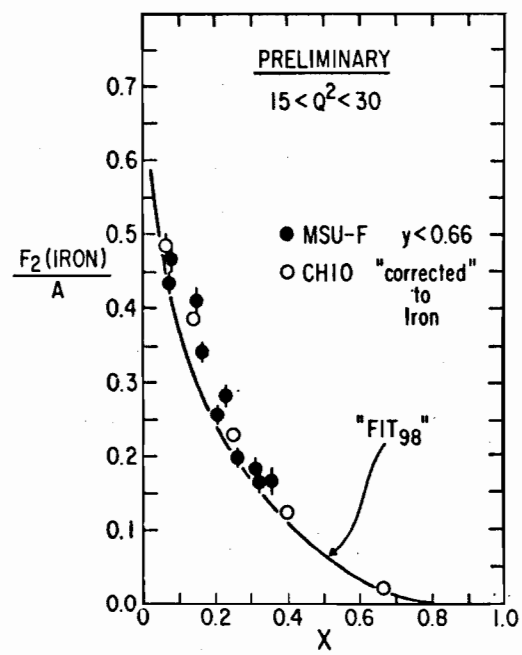

Fig. 13. MSU-F data. Structure function per nucleon.

Below Q^2 = 50 GeV^2 the agreement with the measurements of other groups is quite good, especially when the systematic errors not shown in the Figures are included. These amount to

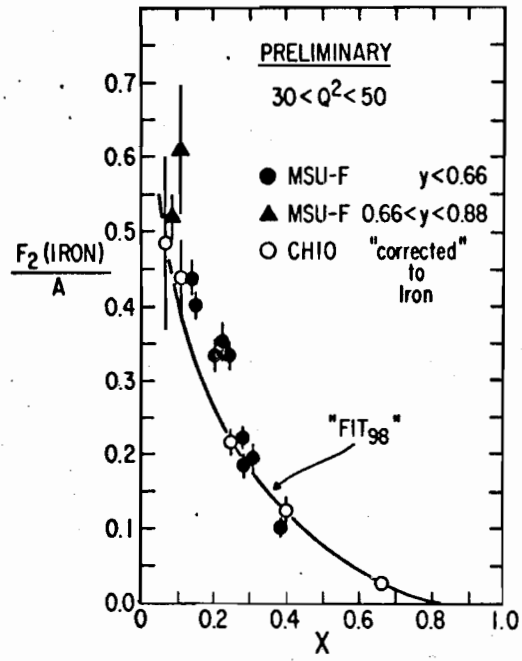

Fig. 14. MSU-F data. Structure function per nucleon.

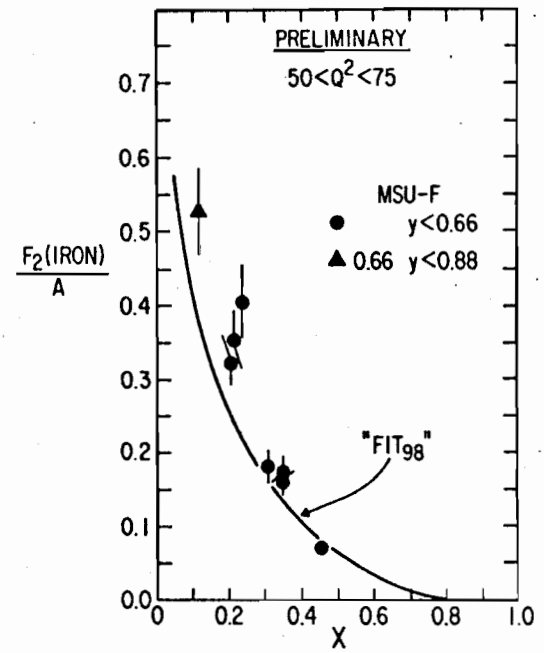

Fig. 15. MSU-F data. Structure function per nucleon.

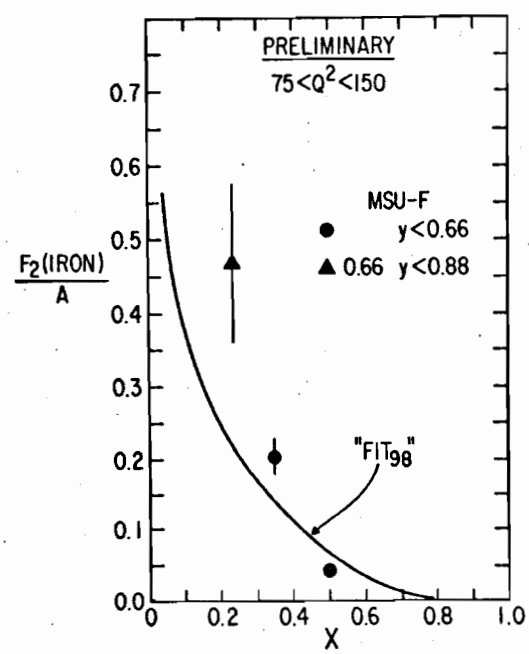

Fig. 16. MSU-F data. Structure function per nucleon.

an estimated 10% for MSU-F and 7% for CHIO. This means, among other things, that the general pattern of scale breaking previously discussed is again confirmed.

On the other hand the agreement is not perfect. Below $Q^2 = 15\ \mathrm{GeV}^2$, at low x, the MSU-F results lie systematically below the CHIO points while at $Q^2 \sim 40\ \mathrm{GeV}^2$ they lie systematically above them. Furthermore, to the extent that the curve represents a valid extrapolation of the lower Q^2 results, this trend seems to continue up to $Q^2 \sim 150\ \mathrm{GeV}^2$ where the MSU-F data is 1 to 2 standard deviations above this curve at low x and 1 to 2 below at high x.

This hints at the tantalizing possibility that the scale breaking effects may become somewhat larger at high Q^2. There is certainly no evidence that they are becoming smaller. Since MSU-F is alone in the region above $Q^2 \sim 50$ GeV^2, we can only wait and see what occurs as the analysis becomes final and the other 85% of the data is included. Only one thing is certain. Whatever develops is sure to spark more theoretical and experimental work on this interesting and important process.

REFERENCES

1. Members of the CHIO Collaboration are: H. L. Anderson, V. K. Bharadwaj, N. E. Booth, R. M. Fine, W. R. Francis, B. A. Gordon, R. H. Heisterberg, R. G. Hicks, T. B. W. Kirk, G. I. Kirkbride, W. A. Loomis, H. S. Matis, L. W. Mo, L. C. Myrianthopoulos, F. M. Pipkin, S. H. Pordes, T. W. Quirk, W. D. Shambroom, A. Skuja, M. A. Staton, W. S. C. Williams, L. J. Verhey, Richard Wilson, and S. C. Wright.

2. Members of the MSU-F Collaboration are: B. Ball, D. Bauer, C. Chang, K. W. Chen, A. Van Ginneken, S. Hansen, J. Kiley, I. Kostoulas, A. Kotlewski, L. Litt, and P. Schewe.

3. E. D. Bloom et al., Phys. Rev. Lett. 23, 930 (1969); M. Breidenbach et al., Phys. Rev. Lett. 23, 935 (1969).

4. J. D. Bjorken, Phys. Rev. 179, 1547 (1969).

5. E. D. Bloom and R. Gilman, Phys. Rev. D4, 2901 (1971); R. E. Taylor, in Proceedings of International Symposium on Lepton and Photon Interactions at High Energies, Stanford, 1975, edited by W. T. Kirk (Stanford Linear Accelerator Center, Stanford, Calif., 1975), p. 679.

6. D. J. Fox et al., Phys. Rev. Lett. 33, 1504 (1974); Y. Watanabe et al., Phys. Rev. Lett. 35, 898 (1975).

7. Wu-Ki Tung, Phys. Rev. Lett. 35, 490 (1975).

8. D. J. Gross and W. Wilzek, Phys. Rev. Lett. 30, 1346 (1973); H. D. Politzer, Phys. Rev. Lett. 30, 1346 (1973).

9. H. L. Anderson et al., Phys. Rev. Lett. 38, 1433 (1977).

10. E. M. Riordan et al., Report No. SLAC-PUB-1634, Stanford Linear Accelerator Center (August 1975).

11. L. Hand, in Proceedings of the International Symposium on Lepton and Photon Interactions at High Energies, Hamburg, 1977 (to be published).

12. S. Stein, et al., Phys. Rev. D12, 1884 (1975).

13. D. H. Perkins et al., CERN/EP/PHY 777, (to be published).

14. E. M. Riordan et al., Phys. Rev. Lett. 33, 561 (1974).